Pergamon

Tetrahedron Vol. 51, No. 25, pp. 7045-7062, 1995

0040-4020/95 $9.50+0.00

0040-4020(95)00335-5

Ab initio Study of the Effect of *N*-Substituents on Properties of Pyrazoles

Otilia Mó,[a] Manuel Yáñez,[a] Antonio L. Llamas-Saiz,[b] Concepción Foces-Foces[b] and José Elguero[c]

[a]Departamento de Química, C-IX, Universidad Autónoma de Madrid, Cantoblanco, 28049 Madrid, Spain

[b]Departamento de Cristalografía, Instituto de Química-Física "Rocasolano", CSIC, Serrano, 119, 28006 Madrid, Spain

[c]Instituto de Química Médica (C.S.I.C.), Juan de la Cierva, 3. 28006 Madrid, Spain

Abstract.— A series of fourteen derivatives of pyrazole have been calculated at the MP2-6-31G** level. The first thirteen are derivatives of the parent pyrazole with different substituents on the nitrogen N(1) and the last one is pyrazole *N*-oxide. The substituents have been selected to cover a wide range of electronic effects. The theoretical results are discussed in relation with geometries, energies, vibrational spectra, Bader analysis and tautomerism (in the case 1-hydroxypyrazole/pyrazole *N*-oxide).

INTRODUCTION

One of the keystones of organic chemistry is related to the effect of substituents on the properties of aromatic rings.[1] In the case of benzene, this led to Hammett equation[2] and to the extraordinary development of Physical Organic Chemistry.[3] It appears that all this enormous amount of work concerns **exclusively** the effect of substituents linked to aromatic rings through the C (aromatic and heteroaromatic compounds all together). We have found of interest to study the effect of substituents through the N atom and for this purpose we have selected pyrazoles.

Two of our previous works are worth mentioning. First, a statistical survey of the X-ray structures of pyrazoles, where the geometries were classified according to the nature of the substituent on N(1).[4] Then, a theoretical study of pyrazole itself where the quality of the different basis sets was explored using as criteria the geometry and rotational constants.[5]

The studied pyrazoles are represented below; the numbering follows the atomic number of R.

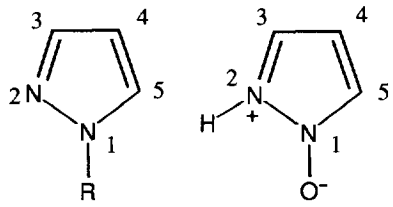

1-13 **14**

1. *N*-H; **2**. *N*-BH_2; **3**. *N*-BH_3^-; **4**. *N*-CH_3; **5**. *N*-CHO; **6**. *N*-CF_3; **7**. *N*-NH_2; **8**. *N*-NO_2; **9**. *N*-OH; **10**. *N*-AlH_2; **11**. *N*-SiH_3; **12**. *N*-PH_2; **13**. *N*-SO_2H; **14**. *N*-oxide. The groups were selected because there is information of the corresponding pyrazoles although in some cases the substituent has been greatly simplified; for instance, BH_3^- for polypyrazolylborates, CHO for azolides, etc. The information we were looking for is mainly geometrical and in most cases came from crystallography.

RESULTS AND DISCUSSION

The geometries are represented in Fig. 1. Additional data are provided for the C-H protons (Table 1) and for N-R substituents (Table 2).

Table 1. Geometrical parameters related to CH bonds (Å, degrees)

	C(3)-H(3)		C(4)-H(4)		C(5)-H(5)	
Comp.	bond length	N(2)-C(3)-H(3)	bond length	C(3)-C(4)-H(4)	bond length	N(1)-C(5)-H(5)
1	1.077	119.1	1.076	128.2	*1.073*	*121.9*
2	1.078	119.4	1.076	127.8	1.077	120.5
3	*1.081*	*119.4*	*1.079*	*128.6*	*1.078*	*120.1*
4	1.078	119.2	1.076	128.2	1.077	121.4
5	1.078	119.3	1.076	*127.8*	1.076	120.8
6	1.077	119.0	1.076	128.1	1.075	121.8
7	1.078	119.2	1.076	128.0	1.075	120.7
8	*1.076*	*118.8*	*1.075*	128.0	1.073	121.8
9	1.076	119.0	1.076	128.1	1.075	121.6
10	1.078	119.4	1.076	127.9	*1.078*	121.1
11	1.078	119.3	1.076	128.0	1.077	121.4
12	1.078	119.0	1.076	128.1	1.077	121.1
13	1.078	119.0	1.076	127.8	1.075	121.3
D[a]	0.005	0.6	0.004	0.8	0.005	1.8
14	1.075	121.2	1.075	126.2	1.074	118.5

[a] Difference between extreme values (indicated in the table in italics)

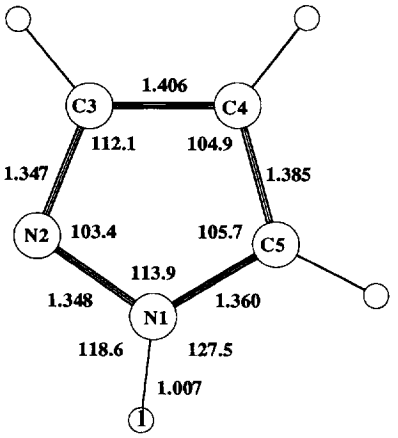

1

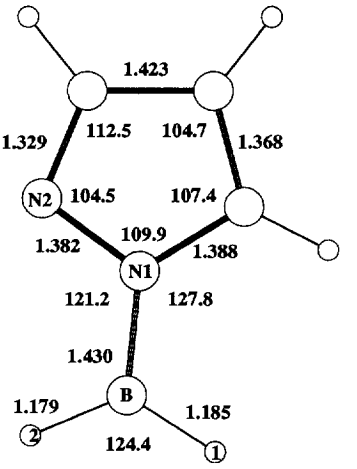

τ(N2-N1-B-H2)=0.0
τ(N2-N1-B-H1)=180.0

2

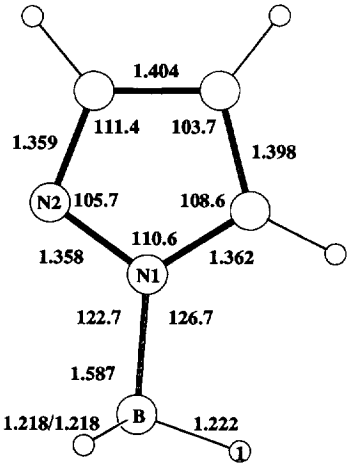

τ(N2-N1-B-H1)=180.0
τ(N2-N1-B-H2)=−60.7
τ(N2-N1-B-H3)=60.7

3

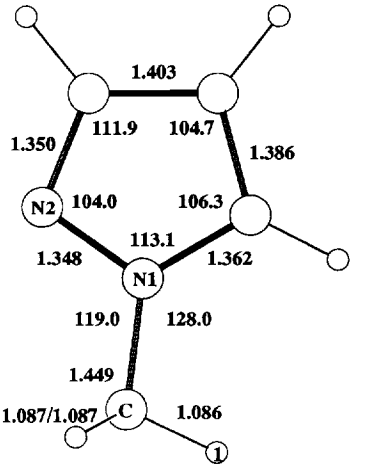

τ(N2-N1-C-H1)=180.0
τ(N2-N1-C-H2)=−60.0
τ(N2-N1-C-H3)=60.0

4

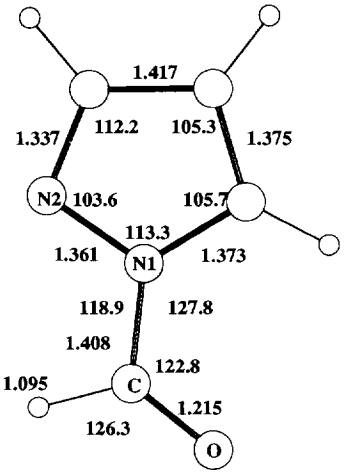

τ(N2-N1-C-O)=180.0

5

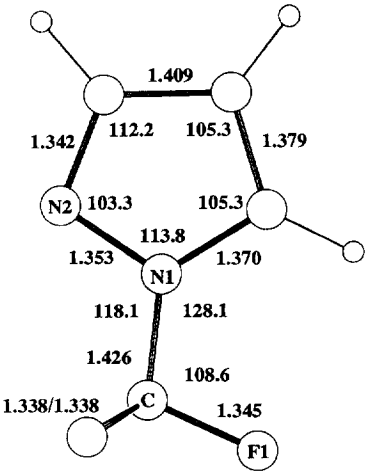

τ(N2-N1-C-F1)=180.0
τ(N2-N1-C-F2)=–60.3
τ(N2-N1-C-F3)=60.3

6

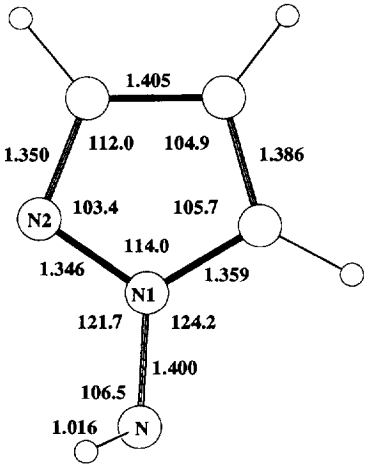

τ(N2-N1-N-H1)=56.7
τ(N2-N1-N-H2)=–56.7

7

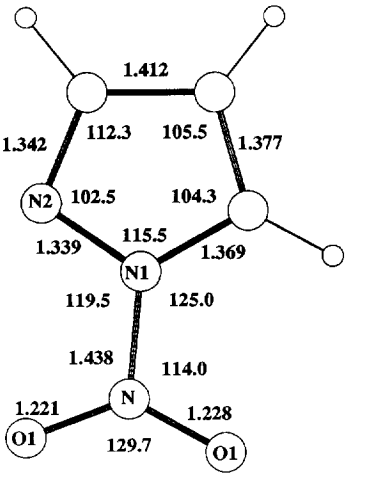

τ(N2-N1-N-O1)=180.0
τ(N2-N1-N-O2)=0.0

8

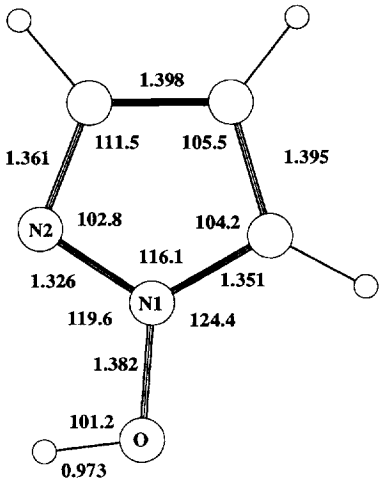

τ(N2-N1-O-H)=0.2

9

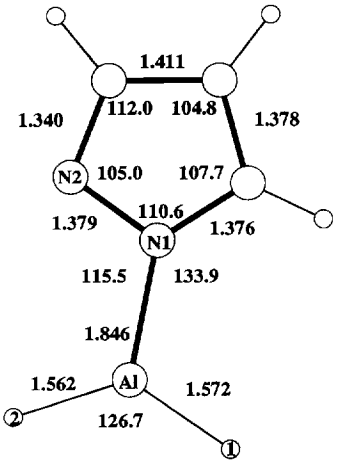

τ(N2-N1-Al-H1)=180.0
τ(N2-N1-Al-H2)=0.0

10

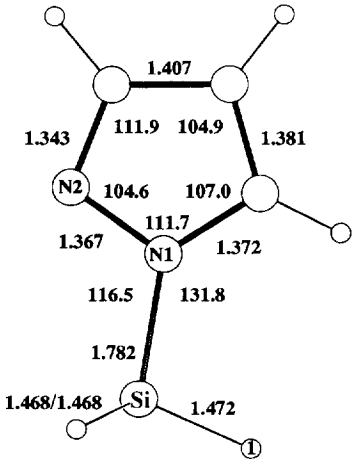

τ(N2-N1-Si-H1)=180.0
τ(N2-N1-Si-H2)=−60.8
τ(N2-N1-Si-H3)=60.8

11

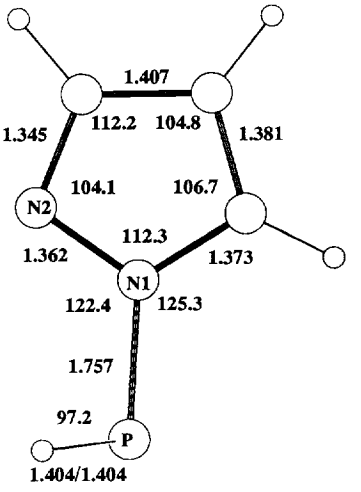

τ(N2-N1-P-H1)=47.9
τ(N2-N1-P-H2)=−47.9

12

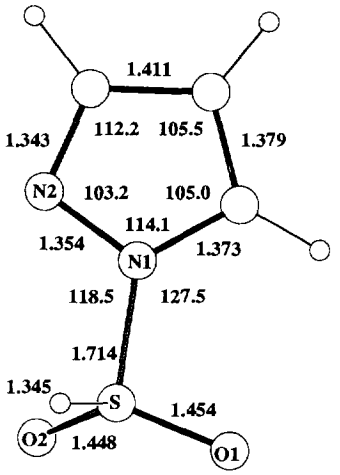

13

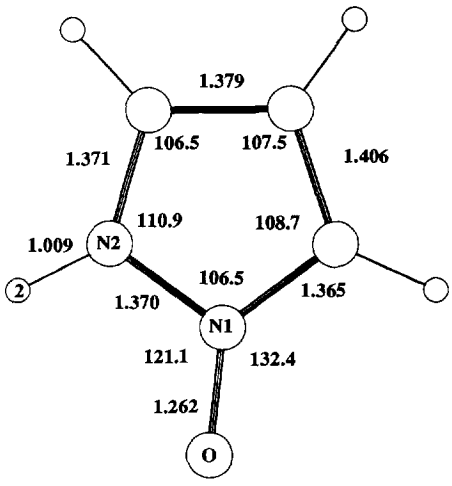

14

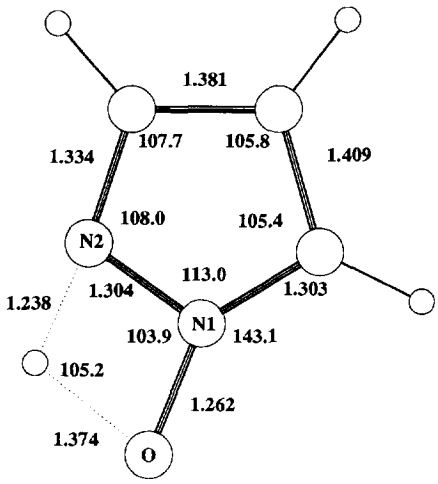

$TS^{\#}$

Fig. 1. MP2-6-31G** geometries of N-substituted pyrazoles (Å, °).

Table 2. Bond angles (degrees) related to the substituent

Comp.	Substituent on N(1)						
2	BH_2	N(1)-B-H(1)	117.0	N(1)-B-H(2)	118.6	H(1)-B-H(2)	124.4
3	BH_3^-	N(1)-B-H(1)	105.5	N(1)-B-H(2)	108.6	N(1)-B-H(3)	108.6
		H(1)-B-H(2)	111.2	H(1)-B-H(3)	111.2	H(2)-B-H(3)	111.5
4	CH_3	N(1)-C-H(1)	108.5	N(1)-C-H(2)	109.7	N(1)-C-H(3)	109.7
		H(1)-C-H(2)	109.8	H(1)-C-H(3)	109.8	H(2)-C-H(3)	109.4
5	CHO	N(1)-C-O	122.9	N(1)-C-H	110.9	H-C-O	126.2
6	CF_3	N(1)-C-F(1)	108.6	N(1)-C-F(2)	111.2	N(1)-C-F(3)	111.2
		F(1)-C-F(2)	108.8	F(1)-C-F(3)	108.8	F(2)-C-F(3)	108.1
7	NH_2	N(1)-N-H(1)	106.5	N(1)-N-H(2)	106.5	H(1)-N-H(2)	106.6
8	NO_2	N(1)-N-O(1)	116.2	N(1)-N-O(2)	114.0	O(1)-N-O(2)	129.7
10	AlH_2	N(1)-Al-H(1)	119.3	N(1)-Al-H(2)	114.0	H(1)-Al-H(2)	126.7
11	SiH_3	N(1)-Si-H(1)	104.8	N(1)-Si-H(2)	109.6	N(1)-Si-H(3)	109.6
		H(1)-Si-H(2)	111.0	H(1)-Si-H(3)	111.0	H(2)-Si-H(3)	110.8
12	PH_2	N(1)-P-H(1)	97.2	N(1)-P-H(2)	97.2	H(1)-P-H(2)	94.9
13	SO_2H	N(1)-S-O(1)	109.1	N(1)-S-O(2)	104.7	N(1)-S-H	97.3
		O(1)-S-O(2)	124.1	O(1)-S-H	108.2	O(2)-S-H	110.0
14	*N*-oxide	N(1)-N(2)-H(2)	116.1	C(3)-N(2)-H(2)	133.0		

To compare experimental as well as calculated geometries for pyrazoles we have used Paul-Curtin plots.[4,5] These two-dimensional plots (see Fig. 2) are differences in bond angles *vs* differences in bond lengths. One of the plots represents $\Delta(N)$ = N(2)-N(1)-C(5) - N(1)-N(2)-C(3) (in degrees) *vs* $\Delta R(NC)$ = N(1)-C(5) - N(2)-C(3) (in hundredths of Å); the other uses $\Delta(C)$ = N(2)-C(3)-C(4) - N(1)-C(5)-C(4) (in degrees) *vs* $\Delta R(CC)$ = C(3)-C(4) - C(4)-C(5) (in hundredths of Å)

Now the geometries of Fig. 1 can be compared with those reported in ref. 4. Two new data have appeared since then. The microwave (MW) geometry of 1-nitropyrazole **8** has been determined[6] as well as the X-ray structure of 1-hydroxypyrazole **9**.[7] As far as compound **8** is concerned we have already shown the excellent quality of MP2-6-31G** calculations to reproduce MW geometries; the experimental X-ray structure of **9** has been determined recently by Begtrup *et al.*[7] The main difference is the conformation of the OH group, almost perpendicular to the pyrazole plane, but this difference is a consequence of the packing of the compound: a tetramer formed by molecules with intermolecular hydrogen bonds between the OHs and the N(2) atoms. Otherwise, the geometries are very similar, even the most singular fact of this structure, the fact that $100x\Delta R(CC)$ is negative, is well reproduced: X-ray = -1.2, MP2-6-31G** = -1.0.

Some interesting features regarding the structure of the substituents along the series should be singled out for comment. It can be observed for instance that while the BH_2 and AlH_2 substituents are coplanar with the pyrazole ring, this is not the case when the substituents are NH_2 and PH_2, where the two hydrogen atoms are in a plane perpendicular to the pyrazole ring (the so-called "parallel conformation", experimental and theoretically the most stable in the case of 1-aminopyrazole).[8,9] This is the result of the strong repulsion between the lone-pair at the N(2) atom and those of the substituents in the latter two cases, and which are not present when the substituents are BH_2 or AlH_2. On the other hand, as we shall discuss later, a coplanar conformation of the BH_2 and AlH_2 substituents will favour a significant stabilization of the azole system by a π-charge transfer to the appropriate vacant orbitals of the substituent. The most stable conformation of compound **5** is a consequence of

the stabilizing interactions between the negatively charged oxygen atom and the C(5)-H proton and between the hydrogen of the substituent and the N(2) lone pair. Similar reasonings permit to explain the local configurations of CF_3 and OH substituents. It can be also observed that the pyramidalization of the NH_2 is much smaller than that found for the PH_2 substituent. This is a well-known difference between this first and second row atoms, reflected in much higher inversion barrier for phosphorus containing compounds.[10] Finally, it may be observed that, as is well known, in pyrazole the N(1)-H group presents a clear tilt toward the N(2). This is a consequence of the different *p* character of the hybrid orbitals involved in the N(1)-C(5) and N(1)-N(2) bonds, respectively. Quite interestingly, this tilt does not change significantly upon substitution with four exceptions: R = NH_2, PH_2, AlH_2 and SiH_3. In the first two cases the tilt is considerably smaller than that found in the parent compound, while in the latter two it is significantly greater. In the first two cases, as we have mentioned above the lone pair of the substituents are pointing away from the lone pair of the N(2) atom, favouring an attractive interaction of the former with the positively charged C(5)-H hydrogen atom. As a result of this non-bonding interaction the C(5)-N(1)-R and the N(2)-N(1)-R angles become smaller and larger, respectively, than in the parent compound.

For AlH_2 and SiH_3 the considerably large tilt found is, very likely, a direct consequence of the electropositive character of both central atoms. Actually, in both compounds the net positive charges at the aluminium and silicon atoms are considerably large (+0.82 and +0.93, respectively). Hence, one may expect an attractive interaction between these positive charges and the N(2) lone pair, which would result in an increase of the tilt. It may be also observed that this tilt is likely responsible for the rocking of the substituents, since the local symmetry axes of the substituent do not coincide with the N(1)-R bond axes. Taking the case of R = BH_2 as a suitable example, it may be observed, for instance, that the N(1)-B-H(1) bond angle is about 6° greater than the N(1)-B-H(2) one.

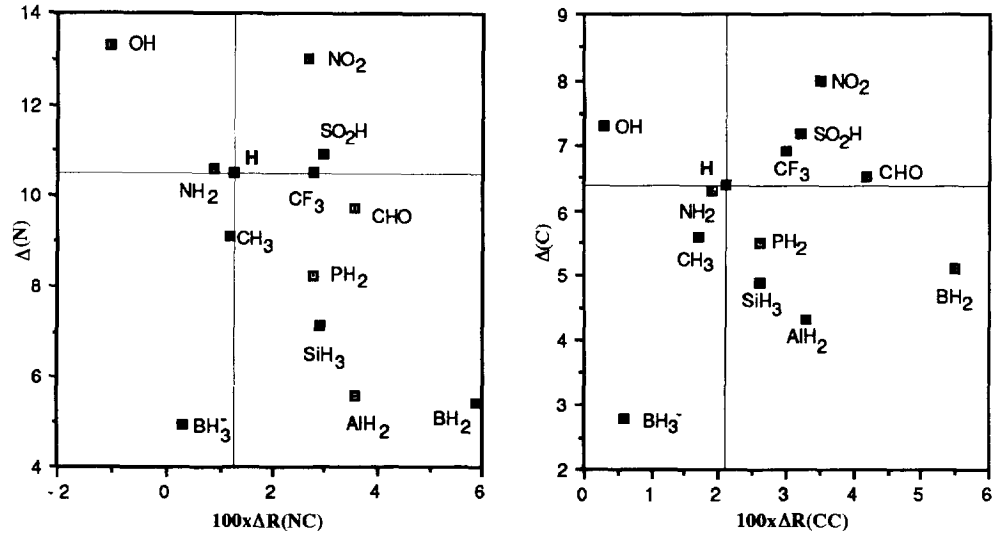

Fig. 2. Paul-Curtin's diagram of N-substituted pyrazoles

Figure 2 represents the geometry of *N*-substituted pyrazoles using the Paul-Curtin's plots. The clustering of the substituents is similar to a representation of inductive *vs* resonance effects (for instance of σ_I vs σ°_R, Fig. 3a): **I**, H, NH_2, CH_3; **II**, OH; **III**, BH_3^-; **IV**, NO_2, SO_2H, CF_3, CHO; **V**, PH_2, SiH_3, AlH_2, BH_2. Only the hydroxy group shows a different behaviour, in a σ_I vs σ°_R plot, it is much more close to the amino group. This observation corresponds to a sizeable effect of the substituent on the N(2)-N(1)-C(5) endocyclic angle. In general, electron withdrawing substituents such as NO_2 or OH produce a widening of this angle, while the opposite effect is found for electropositive groups such as BH_2, AlH_2 or SiH_3. These changes may be explained in terms of hybridization changes induced by the substituent at N(1). Electron withdrawing substituents favour a greater *p* character of the hybrid involved in the N(1)-R linkage; by orthogonality the hybrids involved in the N(1)-C(5) and N(1)-N(2) bonds increase their *s* character and, consequently, the N(2)-N(1)-C(5) angle increases. The opposite mechanism may be invoked in the cases of BH_2, AlH_2 and SiH_3 substituents.

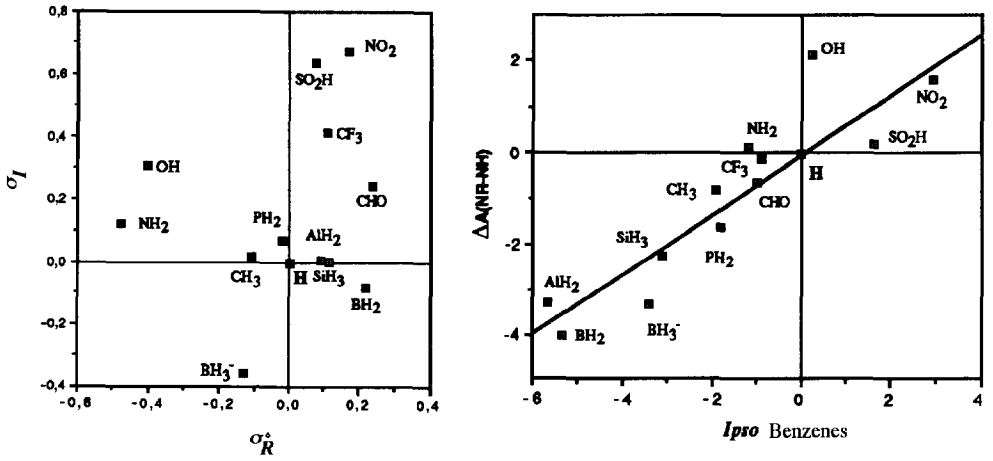

Fig. 3. a) σ_I *vs* σ°_R for aromatic substituents; b) N(2)-N(1)-C(5) angle (NR-NH) *vs ipso* angle in benzenes (CR-CH)

Since there is a relationship between properties of *N*-substituted pyrazoles (Fig. 2) and properties of benzenes (Fig. 3a), we have represented in Fig. 3b a graph of the effect of substituents through the nitrogen *vs* the effect of substituents through the carbon (*ipso* effect). The last values are those from Domenicano and Murray-Rust[11] with some additional values for the less common substituents retrieved from the CSD.[12] The relationship is quite satisfactory, taking into account that *ipso* angular effects came from crystal structures not identical to those calculated (PPh_3 instead of $PhPH_2$, BPh_4^- instead of $Ph\text{-}BH_3^-$ and so on). The regression line ($r = 0.94$) does not include the point corresponding to the OH group.

The effect of the different substituents on the structure of the pyrazole ring is quite significant in some cases (BH_2, OH) while it is small in some others. These effects can be rationalized in terms of the electronic properties of the substituent. For instance BH_2 is a σ-donor group, hence, according to the arguments mentioned above, if the N1 hydrogen atom of pyrazole is replaced by a BH_2 group the N1 valency towards the B atom has less *p* character than it had towards the hydrogen. This implies an increase in the *p* character of the other two N1

hybrid orbitals, which leads to a decrease in the angle between them, to an increase of the N1-N2 and N1-C5 bond lengths and to a decrease in the distal N2-C3 and C5-C4 bonds. Furthermore, BH_2 is the best π-acceptor, hence there is an additional π-charge transfer from the azole system to the substituent, which contributes to increase further the N1-C5 and the N1-N2 bond lengths. Similar effects, although smaller, are observed for second-row substituents (AlH_2, SiH_3) which are also σ-donors and π-acceptors (the latter through a hyperconjugation effect). These charge redistributions are mirrored in the shifting of the harmonic vibrational frequencies, which will be presented in a forthcoming paper,[13] and in the topology of the corresponding charge densities (see Table 5). It can be seen, for instance, that BH_2 substitution implies a sizeable decrease in the charge densities at the N1-N2 and N1-C5 bond critical points, while those at the N2-C3 and C4-C5 clearly increase. Similar changes, although smaller, are found upon AlH_2 and SiH_3 substitution. The significant π-charge transfer from the azole system to the substituent is also reflected in a sizeable ellipticity of the corresponding N-R linkages.

The effects of substituents such as CHO are a composite of σ-acceptor and π-acceptor abilities. Due to the poorer σ-acceptor ability of the formyl group, its π-acceptor effect dominates and a lengthening of the N1-N2 and N1-C5 bonds and a shortening of the N2-C3 and C4-C5 bonds are observed. CF_3 and NO_2 substituents behave also as σ- and π-acceptors, both effects being now significantly important. Since both effects on the pyrazole ring are of opposite sign, the geometry does not change much upon substitution. NH_2 and OH belong to the group of substituents that behave as σ-acceptors and π-donors. Therefore they lead to a shortening of the N1-N2 and N1-C5 bonds and to a lengthening of the distal N2-C3 and C4-C5 bonds. These effects are particularly important upon OH substitution since this group is the best σ-acceptor considered in this study. Although NH_2 should be a better π-donor than OH, leading also to a significant shortening of the N1-N2 and N1-C5 bonds, it can be seen that in this case the geometrical effects are less pronounced. This is due to the fact, mentioned above, that in the most stable conformation, the lone pair of the amino group lies in the plane of the molecule and the conjugation with the π-azole system is only of a hyperconjugative type. Again, this is reflected in the charge distribution of the corresponding derivatives (see Table 5), which shows that the charge densities at the N1-N2 and N1-C5 bond critical points of the NH_2 derivative are only slightly greater than for pyrazole itself.

We have considered also of interest to analyze the stabilization effects of the substituents on the pyrazole system. For this purpose, we shall use the so called "methyl stabilization energies", defined as the enthalpy of the reaction: PzR + CH_4 → PzH + RCH_3 (PzR is an *N*-R substituted pyrazole).

These methyl stabilization energies have proved[14] to be a reliable tool to analyze energy data from theoretical calculations. For the sake of consistency, the structures and the ZPE of the corresponding methyl derivatives (RCH_3) were optimized at the MP2-6-31G** level of theory. ZPE were scaled by the empirical factor 0.93. The calculated methyl stabilization energies are summarized in Table 3.

Table 3. MP2/6-31G** Methyl stabilization energies (ΔE in kcal mol^{-1}) of *N*-substituted pyrazoles

R	**2** BH_2	**4** CH_3	**5** CHO	**6** CF_3	**7** NH_2	**8** NO_2	**9** OH	**10** AlH_2	**11** SiH_3	**12** PH_2	**13** SO_2H
	29.6	3.0	12.7	-3.0	-8.0	2.7	-25.0	27.8	15.9	6.3	-1.3

It can be seen that, in general, π-acceptor substituents stabilize the azole system while σ-acceptor and π-donor substituents clearly destabilize it. This likely reflects the fact that azoles are π-excessive systems, which are then stabilized when the delocalization involves also the appropriate orbitals of the substituent. This seems to be ratified by the fact that the best π-acceptor (BH_2) leads to the greater stabilization, while the best σ-acceptor (OH) leads to the greater destabilization. For the particular cases of BH_2, AlH_2 and SiH_3 substituents, the high N^--R^+ polarity is also an important contributor to the enhanced stabilities of these derivatives.

Concerning the *N*-oxide **14**, to be consistent with other pyrazoles, it must be represented with the resonance form **14a** and not with **14b**, that is, with the largest angle on the N-H.

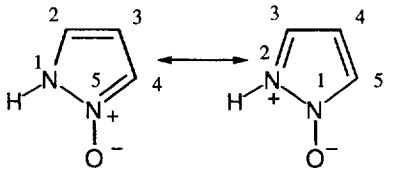

14a **14b**

We have reported in Table 4, the most significant data concerning these compounds, including not only energies but also dipole moments and rotational constants. The data regarding pyrazole **1** and 1-nitropyrazole **8** have been published elsewhere.[5,6]

Table 4. Total energies, E (Hartrees), zero point energies, ZPE (Hartrees), dipole moments, μ (D) and rotational constants, A, B, C (MHz) for *N*-substituted pyrazoles. All values obtained at the MP2-6-31G**//MP2-6-31G** level, with the only exception of ZPE which were obtained at the HF-6-31G** level.

R	E	ZPE	μ[a]	A	B	C
2. BH_2	-250.90505	0.08886	2.27 (2.05, -0.99)	8954.3	4008.4	2768.9
3. BH_3^-	-251.55631[b]	0.09538[c]	6.49 (-2.05, -6. 16)	8936.4	3506.7	2570.8
4. CH_3	-264.71773	0.10635	2.42 (-1.96, 1.42)	8960.4	3721 .4	2673.5
5. CHO	-338.57039	0.08753	1.90 (0.51, -1.82)	8218.4	2193.1	1731.1
6. CF_3	-561.77617	0.08281	2.56 (-1.50, 2.07)	3510.4	1316.4	1151.9
7. NH_2	-280.70697	0.09555	0.96 (0.53, 0.80)	9138.8	3789.4	2717.2
9. OH	-300.51133	0.08120	0.58 (0.00,0.58)	9311.2	3846.5	2722.0

10. AlH_2	-468.10266	0.07988	1.83 (1-50, 1.05)	8792.6	2143.8	1723.6
11. SiH_3	-515.72997	0.09308	1.99 (0.63, 1.89)	8511.6	2131.8	1739.4
12. PH_2	-566.94472	0.08539	1.29 (1.07, 0.72)	8803.2	2143.3	1749.4
13. SO_2H	-773.16975	0.08861	3.10 (-2.28, 1.21, 1.72)	4457.5	1366.4	1107.1
14. *N*-Oxide	-300.49547	0.08098	3.82 (-3.55, -1.42)	9254.4	3907.6	2747.5

[a] The values within parentheses correspond to the x and y components. For the particular case of R = SO_2H the z component is different from zero and is also given. [b]Value obtained at the MP2-6-31+G** level. [c]Value obtained at the HF-6-31++G** level.

We have reported in Table 5 the results of the Bader analysis. Part of these data have been discussed in the preceding section, here we will report only a discussion based on ρ_{CC} [charge density in *e* au^{-3} at the bond critical points of the C(3)-C(4) and C(4)-(C)5 bonds]. Considering that there are linear relationships between bond-order and bond-length,[15] between bond order and ρ,[16] as well as between bond-order and $J_{(HH)}$ in pyrazoles,[17] we have compared three collections of data: i) the bond lengths of Fig. 1; ii) the ρ values of Table 5 and a collection of $^3J_{(HH)}$ from references 18-20 (the data are not available for **1** due to prototropic tautomerism, nor for **2**, **6**, **10**, **13**, for **3** instead of BH_3^- the coupling constants are those of tris(pyrazol-1-yl)borate, for **5** instead of CHO the experimental coupling constants are those of *N*-acetylpyrazole, for **11** instead of SiH_3 we have data for $Si(CH_3)_3$, and for **12** instead of PH_2 we used $P[N(CH_3)_2]_2$.

For the thirteen *N*-substituted pyrazoles of Table 5 and Fig. 1, the following equation was found by regression:

$$d_{CC} = 1.675 - 0.860\ \rho_{CC},\ n = 26,\ r^2 = 0.954,\ sd = 0.0033 \qquad [1]$$

The maximum deviation is found for the OH and BH_2 substituents; without these substituents, the correlation improves considerably:

$$d_{CC} = 1.665 - 0.829\ \rho_{CC},\ n = 22,\ r^2 = 0.985,\ sd = 0.0018 \qquad [2]$$

Considering that we have coupling constants only for eight compounds, we have repeated the regression for these points:

$$d_{CC} = 1.652 - 0.791\ \rho_{CC},\ n = 16,\ r^2 = 0.945,\ sd = 0.0032 \qquad [3]$$

The maximum deviation is found for the OH substituent (the BH_2 substituent does not belong to this subset); without this substituent, the correlation improves:

$$d_{CC} = 1.663 - 0.825\ \rho_{CC},\ n = 14,\ r^2 = 0.979,\ sd = 0.0021 \qquad [4]$$

For this subset, two other correlations are possible:

$$^3J_{(HH)} = 41.68 - 28.3\ d_{CC},\ n = 16,\ r^2 = 0.675,\ sd = 0.27 \qquad [5]$$

$$^3J_{(HH)} = -5.34 + 23.2\ \rho_{CC},\ n = 16,\ r^2 = 0.684,\ sd = 0.26 \qquad [6]$$

Considering the approximation made with the *N*-substituents and also that the range and precision of $^3J_{(HH)}$ (from 1.5 to 3.1 Hz, error ± 0.05 Hz), equations [5] and [6] are reasonably good.

Table 5. Bonding characteristics of the *N*-substituted pyrazoles included in this work. Values of ρ (*e* au^{-3}) and ellipticities, ε, at the critical points.

R	N(1)-N(2)			N(2)-C(3)			C(3)-C(4)			C(4)-C(5)			C(5)-N(1)			N(1)-R		
	ρ	$\nabla^2\rho$	ε	ρ	$\nabla^2\rho$	ε	ρ	$\nabla^2\rho$	ε	ρ	$\nabla^2\rho$	ε	ρ	$\nabla^2\rho$	ε	ρ	$\nabla^2\rho$	ε
1. H	0.392	-0.931	0.122	0.368	-0.372	0.242	0.311	-0.909	0.235	0.338	-1.067	0.362	0.327	-0.305	0.137	0.369	-2.100	0.052
2. BH_2	0.370	-0.862	0.077	0.383	-0.386	0.240	0.302	-0.875	0.181	0.350	-1.129	0.389	0.319	-0.593	0.057	0.199	0.766	0.109
3. BH_3^-	0.398	-0.955	0.136	0.366	-0.606	0.245	0.314	-0.919	0.265	0.326	-0.988	0.308	0.347	-0.522	0.200	0.123	0.560	0.028
4. CH_3	0.395	-0.935	0.137	0.367	-0.399	0.231	0.312	-0.919	0.245	0.336	-1.058	0.353	0.328	-0.292	0.163	0.269	-0.546	0.040
5. CHO	0.380	-0.887	0.091	0.376	-0.325	0.233	0.304	-0.887	0.194	0.347	-1.116	0.381	0.315	-0.354	0.056	0.312	-0.764	0.051
6. CF_3	0.383	-0.885	0.102	0.373	-0.315	0.233	0.308	-0.901	0.210	0.344	-1.109	0.378	0.312	-0.260	0.083	0.328	-1.444	0.080
7. NH_2	0.397	-0.945	0.153	0.366	-0.385	0.227	0.312	-0.915	0.245	0.337	-1.064	0.352	0.329	-0.231	0.149	0.354	-0.847	0.037
8. NO_2	0.383	-0.887	0.083	0.375	-0.285	0.230	0.304	-0.886	0.186	0.349	-1.139	0.389	0.303	-0.171	0.040	0.380	-1.000	0.249
9. OH	0.409	-0.995	0.160	0.361	-0.356	0.228	0.314	-0.923	0.257	0.334	-1.050	0.346	0.325	-0.727	0.182	0.376	-0.861	0.077
10. AlH_2	0.371	-0.849	0.091	0.376	-0.414	0.238	0.307	-0.899	0.213	0.343	-1.084	0.369	0.326	-0.585	0.096	0.086	0.629	0.173
11. SiH_3	0.376	-0.860	0.104	0.373	-0.390	0.234	0.309	-0.905	0.219	0.341	-1.083	0.368	0.323	-0.479	0.103	0.115	0.656	0.107
12. PH_2	0.378	-0.865	0.110	0.373	-0.394	0.231	0.309	-0.905	0.219	0.342	-1.091	0.369	0.322	-0.432	0.099	0.147	0.516	0.056
13. SO_2H	0.375	-0.847	0.086	0.374	-0.308	0.225	0.306	-0.896	0.199	0.346	-1.121	0.383	0.306	-0.286	0.043	0.225	0.029	0.080
14. *N*-oxide[a]	0.404	-1.024	0.290	0.313	-1.692	0.116	0.342	-1.082	0.392	0.309	-0.911	0.235	0.344	0.193	0.386	0.444	-0.711	0.054

[a]N(2)-H(2), ρ = 0.361, $\nabla^2\rho$ = -2.082, ε = 0.051.

The N-OH/N-O Tautomerism of 1-Hydroxypyrazole

The tautomerism 1-hydroxypyrazole **9**/pyrazole *N*-oxide **14** has been studied in the literature. All data are consistent with the predominance of tautomer **9**, both in solution[21,22] and in the solid state.[7] According to the energy values of Table 3, the 1-hydroxy tautomer is more stable than the *N*-oxide by 16 kcal mol^{-1}. These tautomers are separated by a transition state corresponding to an intramolecular transfer of the proton TS‡ = -299.59676 Hartrees (its geometry is represented in Fig. 1), that is, 55.1 kcal mol^{-1} higher than the most stable tautomer. This is a very high energy for an intramolecular proton transfer, and it means that probably the process is forbidden and also that when it takes place, at least in solution, the mechanism is probably intermolecular (dimers- or solvent-assisted). In the related case of 2-hydroxy-3-methylindazole, where both tautomers are present in appreciable amounts in solution, the equilibrium is fast enough to be observe, for the mixture of tautomers, only average signals in ^{13}C and ^{15}N NMR spectroscopy [see also ref. 22].[23]

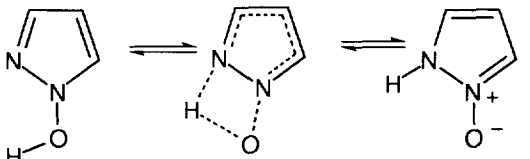

9 **TS$^{\#}$** **14**

Computational Details

Ab initio molecular orbital calculations were performed using the Gaussian-90 and Gaussian-92 series of programs.[24] The geometries of the *N*-substituted pyrazoles under investigation were fully optimized at the Hartree-Fock level of theory using a 6-31G** basis set.[25] The harmonic vibrational frequencies were calculated using analytical second derivative techniques in order to check whether the optimized structures are minima of the potential energy surface, and to evaluate the corresponding zero point energies. A detailed discussion of the harmonic vibrational frequencies will be presented elsewhere.

We have recently shown that the rotational constants are a tight criterion to define the quality of a molecular geometry.[5] In the same reference, taking pyrazole as a bench mark case, it was also found that, when this criterion is invoked, the MP2-6-31G** geometries are quite reliable, yielding rotational constants which deviate, in average, by 0.03 % from the experimental ones. For this reason the HF-6-31G** structures were refined at the MP2-6-31G** level. For the particular case of *N*-BH_3^- pyrazole the HF geometry was obtained using a 6-31++G** basis set, since it is well known that a proper description of anionic systems requires the inclusion of diffuse components in the basis set. This HF geometry was then refined at the MP2-6-31+G** level.

The total energies, as well as the ZPE energies, the dipole moments and the rotational constants have been summarized in Table 3. Since information on the direction of the dipole moment can be of some relevance, the non-zero components are also given in this Table. It should be mentioned that the dipole moments were evaluated at the MP2 level to take into account electron correlation effects on the value of this one-electron

property. Actually, we have found, for some of the systems investigated, differences up to 0.8 D between HF and MP2 dipole moments.

Both the characteristics of the bond between the pyrazole N(1) nitrogen and the substituent, and the charge redistribution induced by the substituent on the pyrazole system, will be discussed taking advantage of the topological analysis of the electronic charge density and its Laplacian.[26] The Laplacian of the electron density $[\nabla^2\rho(\mathbf{r})]$ identifies regions of space wherein $\rho(\mathbf{r})$ is locally concentrated ($\nabla^2\rho < 0$) or depleted ($\nabla^2\rho > 0$). Therefore a negative value of ($\nabla^2\rho(\mathbf{r})$) in the internuclear region of two interacting atoms implies the formation of a typical covalent bond, since electron density is built up in that region. On the contrary, positive values of the Laplacian are characteristic of the interaction between closed shell systems where the charge is depleted from the internuclear region and concentrated on the corresponding atomic basins. A topological analysis of the Laplacian also provides interesting information on charge redistributions upon substitution. If the Laplacian within a bonding region becomes more negative, this may be taken as an indication of a reinforcement of the bond, since more electronic charge is concentrated in that region. On the contrary, if the Laplacian becomes less negative or even positive, a charge depletion took place and the corresponding bond becomes weakened. In this respect, the location of the bond critical points offers a more quantitative information. The bond critical points correspond to stationary points of the electronic charge density where $\rho(\mathbf{r})$ is minimum along the bond path and maximum in the other two directions. The existence of a bond critical point between two atomic basins indicates the existence of a bond. The value of the charge density at the bond critical point (bcp) is a relative measure of the strength of the corresponding linkage.

Some Concluding Remarks

Concerning the transmission of substituent effects we have noted (Fig. 3b) that the OH group behaves abnormally . We also reported (eqs. [1] and [2]) that the OH and BH_2 substituents present some anomalies. In summary, two substituents deserve further attention: BH_2 and OH.

Another aspect concerns aromaticity. Probably, aromaticity needs at least two descriptors,[27-30] but assuming the simplified view that aromaticity is related to bond order (or bond length, see eqs. [1] and [2]),[31] then the more aromatic an N-R pyrazole, the less different the ΔR_{CC} and ΔR_{CN}, in other words, the more regular the pentagon. We have represented in Fig. 4 ΔR_{CN} vs ΔR_{CC} (using values from Fig. 1): the aromaticity increases from BH_2 to OH (just the two abnormal points!). In this respect it is worth remembering that BH_2 and OH are the substituents that stabilize and destabilize the most, respectively, the pyrazole system.

A final comment concerns the methyl stabilization energies of Table 3. These energies are related to the geometries, *i.e.* to the aromaticity of the pyrazole ring. For instance, in the coordinates of Fig. 2 (left side) and Fig. 4, the following multiple-regression equations [7] and [8] are found [all points, including the proton (ΔE = 0) but not the anion BH_3^-]:

$$\Delta E \text{ (Me stab)} = 23.6 - 3.1\ \Delta(N) + 4.5\ [100x\Delta(NC)],\ n = 12,\ r^2 = 0.915,\ sd = 4.96 \quad [7]$$

$$\Delta E \text{ (Me stab)} = -5.1 + 14.3\ [100x\Delta R(NC)] - 8.9\ [100x\Delta R(CC)],\ n = 12,\ r^2 = 0.809,\ sd = 7.31 \quad [8]$$

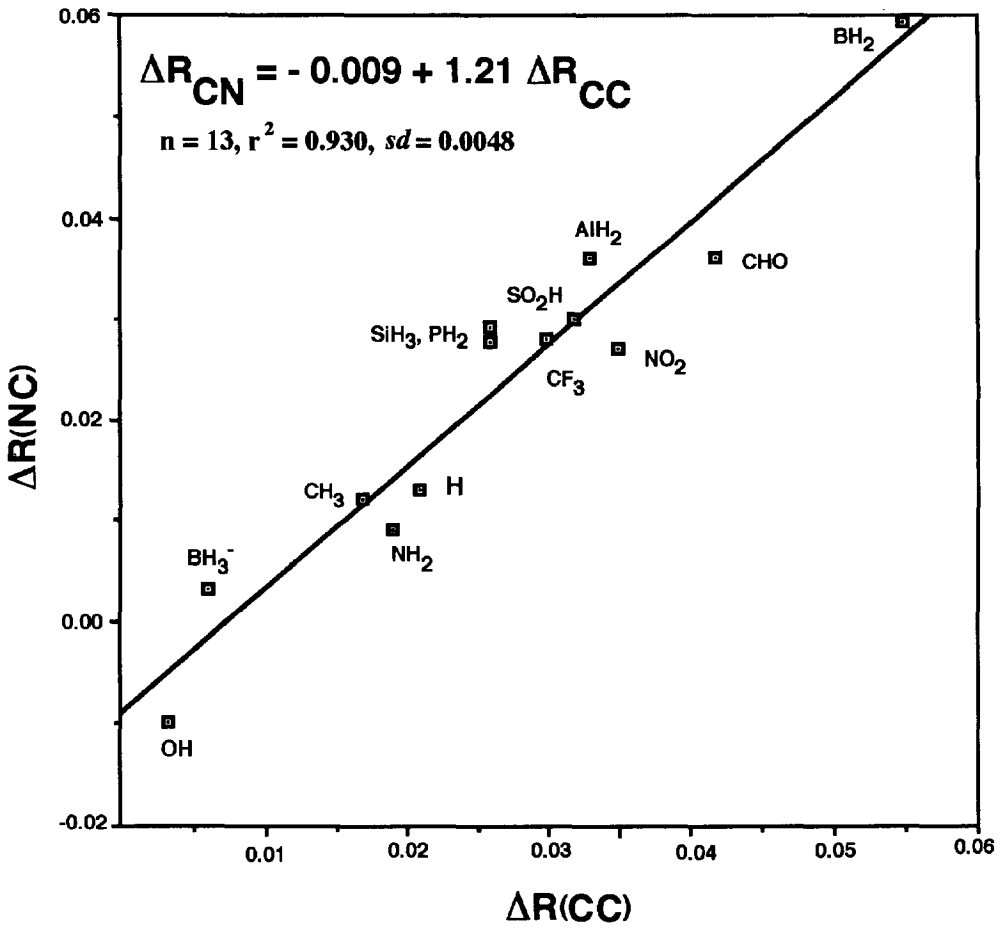

Fig. 4. Plot of ΔR(NC) *vs* ΔR(CC) for the thirteen *N*-substituted pyrazoles

Acknowledgements

Financial support of this work by CICYT (project PB93-0289-C02-01) is gratefully acknowledged. thank Professor Mikael Begtrup (Department of Medicinal Chemistry, Royal Danish School of Pharm Copenhagen, Denmark) for communicating the structure of 1-hydroxypyrazole **9** prior to publication.

References

1. March, J. "Advanced Organic Chemistry", Fourth Edition, John Wiley and Sons, New York, 1992, p. 278.

2. Hammett, L.P. "Physical Organic Chemistry", McGraw-Hill, New York, 1940.

3. Chapman, N.B.; Shorter, J. "Advances in Linear Free Energy Relationships", Plenum Press, London, 1972; Chapman, N.B.; Shorter, J. "Correlation Analysis in Chemistry", Plenum Press, New York, 1978.

4. Llamas-Saiz, A.L.; Foces-Foces, C.; Elguero, J. *J. Mol. Struct.*, **1994**, *319*, 231.

5. Llamas-Saiz, A.L.; Foces-Foces, C.; Mó, O.; Yáñez, M.; Elguero, E.; Elguero, J. *J. Comput. Chem.*, **1995**, *16*, 263.

6. Blanco, S.; López, J.C.; Alonso, J.L.; Mó, O.; Yáñez, M.; Jagerovic, N.; Elguero, J. *J. Mol. Struct.*, **1995**, *344*, 241.

7. Begtrup, M.; Thomsen, H. *to be published.*

8. Foces-Foces, C.; Cano, F.H.; Claramunt, R.M.; Sanz, D.; Catalán, J.; Fabero, F.; Fruchier, A.; Elguero, J. *J. Chem. Soc., Perkin Trans. 2*, **1990**, 237.

9. Claramunt, R.M.; Sanz, D.; Catalán, J.; Fabero, F.; García, N.A.; Foces-Foces, C.; Llamas-Saiz, A.L.; Elguero, J. *J. Chem. Soc., Perkin Trans. 2*, **1993**, 1687.

10. Veillard, A.; Lehn, J.M.; Munsch, B.*Theoret. Chim. Acta*, **1969**, *15*, 225; Levin, C.C. *J. Am. Chem. Soc.*, **1975**, *97*, 5649; Cherry, W.; N. Epiotis, N. *J. Am. Chem. Soc.* **1976**, *98*, 1135; Alcami, M.; de Paz, J.L.G.; Yañez, M. *J. Comput. Chem.*, **1989**, *10*, 468.

11. Domenicano, A.; Murray-Rust, P. *Tetrahedron Lett.* **1979**, 2283.

12. Allen, F.H.; Davies, J.E.; Galloy, J.J.; Johnson, O.; Kennard, O.; Macrae, C.F.; Mitchell, E.M.; Mitchell, G.F.; Smith, J.M.; Watson, D.G. *J. Chem. Inf. Comput. Sci.*, **1991**, *31*, 187.

13. Mó, O.; Yáñez, M.; Elguero, J. in preparation.

14. Hehre, W.J.; Radom, L.; Schleyer, P.V.R.; Pople, J.A. "Ab Initio Molecular Orbital Theory", John Wiley & Sons, New York, 1986.

15. Hosoya, H.; Shobu, M.; Takano, K.; Fujii, Y. *Pure Appl. Chem.* **1983**, *55*, 269.

16. Bader, R.F.W.; Slee, T.S.; Cremer, D.; Kraka, E. *J. Am. Chem. Soc.* **1983**, *105*, 5061.

17. Gready, J.E.; Hatton, P.M.; Sternhell, S. *J. Heterocycl. Chem.* **1992**, *29*, 935.

18. Elguero, J. "Pyrazoles and their Benzo Derivatives", in Comprehensive Heterocyclic Chemistry, Pergamon, Oxford, 1984, **5**, 167.

19. Elguero, J.; Claramunt, R.M.; López, C.; Sanz, D. *Afinidad* **1993**, *50*, 383.

20. Begtrup, M.; Vedsø, P. *J. Chem. Soc., Perkin Trans. 1* **1995**, 243.

21. Elguero, J.; Marzin, C.; Katritzky, A.R.; Linda, P. "The Tautomerism of Heterocycles", Academic Press, New York, 1976, p. 486.

22. Begtrup, M.; Vedsø, P. *to be published.*

23. Schilf, W.; Stefaniak, L.; Webb, G.A. *Magn. Reson. Chem.* **1987**, *25*, 721.

24. Gaussian 90, Revision I, Frisch, M.J.; Head-Gordon, M.; Trucks, G.W.; Foresman, J.B.; Schlegel, H.B.; Raghavachari, K.; Binkley, J.S.; Gonzalez, C.; Defrees, D.J.; Fox, D.J.; Whiteside, R.A.; Seeger, R.; Melius, C.F.; Baker, J.; Martin, R.L.; Kahn, L.R.; Stewart, J.J.P.; Topiol, S.; Pople, J.A. Gaussian Inc., Pittsburgh PA, 1990; Gaussian 92, Revision D.2, Frisch, M.J.; Trucks, G.W.; Head-Gordon, M.; Gill, P.M.W.; Wong, M.W.; Foresman, Johnson, B.G.; J.B.; Schlegel, H.B.; Robb, M.A.; Repogle, E.S.; Gompers, R.; Andres, J.L.; Raghavachari, K.; Binkley, J.S.; Gonzalez, C.; Martin, R.L.; Fox, D.J.; Defrees, D.J.; Baker, J.; Stewart, J.J.P.; Pople, J.A. Gaussian Inc., Pittsburgh PA, 1992.

25. Hariharan, P.C.; Pople, J.A. *Theoret. Chim. Acta*, **1973**, *28*, 213.

26. Bader, R.F.W. Atoms in Molecules. A Quantum Theory. Oxford University Press, New York, 1990.

27. Katritzky, A.R.; Barczynski, P.; Musumarra, G.; Pisano, D.; Szafran, M. *J. Am. Chem. Soc.* **1989**, *111*, 7.

28. Katritzky, A.R.; Feygelman, V.; Musumarra, G.; Barczynski, P.; Szafran, M. *J. Prakt. Chem.* **1990**, *332*, 870.

29. Caruso, L.; Musumarra, G.; Katritzky, A.R. *Quant. Struct.-Act. Relat.* **1993**, *12*, 146.

30. Párkányi, C.; Boniface, C. *Bull. Soc. Chim. Belg.* **1990**, *99*, 587.

31. Bird, C.W. *Tetrahedron* **1985**, *41*, 1409; **1986**, *42*, 89; **1992**, *48*, 335.

(*Received in UK* 22 *March* 1995; *revised* 24 *April* 1995; *accepted* 28 *April* 1995)